Biomass and Bioenergy 81 (2015) 117–128

Contents lists available at ScienceDirect

Biomass and Bioenergy

journal homepage: http://www.elsevier.com/locate/biombioe

Research paper

Abundance and characteristics of lignin liquid intermediates in wood (*Pinus ponderosa* Dougl. ex Laws.) during hot water extraction

Manuel Raul Pelaez-Samaniego [a, b, *], Vikram Yadama [c, d], Manuel Garcia-Perez [a], Eini Lowell [e]

[a] Department of Biological Systems Engineering, Washington State University, Pullman, WA, USA
[b] Faculty of Chemical Sciences, Universidad de Cuenca, Cuenca, Ecuador
[c] Department of Civil and Environmental Engineering, Washington State University, Pullman, WA, USA
[d] Composite Materials and Engineering Center, Washington State University, Pullman, WA 99164, USA
[e] USDA Forest Service, Pacific Northwest Research Station, Portland, OR, USA

ARTICLE INFO

Article history:
Received 29 March 2015
Received in revised form
18 May 2015
Accepted 21 June 2015
Available online xxx

Keywords:
Lignin
Hot water extraction
Ponderosa pine (*Pinus ponderosa* Dougl. ex Laws.)
Pretreatment
Wood

ABSTRACT

The objective of this research was to investigate the effects of the conditions of hot water extraction (HWE) on abundance, properties, and structure of lignin depolymerization products. HWE of extracted softwood (ponderosa pine) was conducted using temperatures from 140 to 320 °C for 90 min. HWE materials were then subjected to a soxhlet extraction process using dichloromethane (DCM). The composition and molecular weight of this DCM-soluble material was conducted using semi-quantitative Py-GC/MS and ESI/MS, which showed that this material is rich in lignin with low molecular weight (<1200 g mol^{-1}) and low polydispersity (~1.4). The highest yield of this material (~4.2%) was obtained in material processed at 260 °C. Py-GC/MS of the solid fraction after the DCM process showed a progressive reduction of products of the pyrolysis of lignin as the HWE temperature increased. This finding suggests that the lignin content in the solid decreased due in part to migration from the cell walls and middle lamella to the particles surfaces, particularly the inner surface of the cells. SEM and AFM techniques helped to visualize the ability of this DCM-soluble extract to adhere to cellulosic fibers. Therefore, this lignin-rich material presents properties that depend on the conditions of the operation. Results indicate that during HWE it is possible to control the process parameters to limit or increase the amount of DCM-soluble lignin and its properties as required for downstream processes.

1. Introduction

Effective pretreatments for fractionating wood are required in an integrated operation to derive an array of products, including wood composites, fuel pellets, liquid fuels, and chemicals. For fuels and chemicals, for example, pretreatment is primarily designed to reduce the inherent recalcitrance of wood carbohydrates to enzymatic hydrolysis. Since lignin negatively affects enzymatic hydrolysis, wood delignification operations are required [1,2]. Reducing lignin content (close to complete elimination) may improve carbohydrates accessibility for enzymatic hydrolysis [2,3]. However, complete delignification could have an adverse effect [4,5]. Thus, it has been suggested that changing lignin composition and structure can be a more appropriate strategy for effective digestibility of lignocellulosic materials [6,7]. For wood composites and fuel pellets, on the other hand, the presence of lignin, especially on the fibers surface, is beneficial for the products' properties [8–13].

Thermal pretreatment operations such as hot water extraction (HWE) and torrefaction can partially degrade/remove hemicelluloses, increase the degree of crystallinity of cellulose, and modify lignin properties [13–15]. HWE has been recognized as a pretreatment method with potential for both biochemical and thermochemical conversion schemes [16–18]. In HWE wood is heated above lignin's glass transition temperature (which can vary from ~80 to 140 °C [19–21] or above, depending, for example, on moisture content). The process is accompanied by lignin-carbohydrate bonds breaking and depolymerization, sometimes followed by condensation reactions [22,23]. Lignin in a rubbery

* Corresponding author. Department of Biological Systems Engineering, Washington State University, Pullman, WA 99164, USA
E-mail addresses: m.r.pelaezsamaniego@email.wsu.edu, manuel.pelaez@ucuenca.edu.ec (M.R. Pelaez-Samaniego).

http://dx.doi.org/10.1016/j.biombioe.2015.06.012
0961-9534/

state and partially depolymerized can coalesce and in part migrate (diffuse) from the wood cell wall and from the middle lamella to the surfaces, especially the inner cell wall surface [19], where it is deposited forming droplets or layers of lignin-rich material [14,24,25]. This material is in a liquid-like reactive state [26,27], forming lignin liquid intermediates (LLI), and is constituted by lignin fragments linked with carbohydrates [28–30]. Similar behavior has been observed in torrefaction [31].

Blends of LLI with thermoplastics during compounding of wood plastic composites appear to impact the rheology of processing the composite [13]. Hardboard produced by the Masonite process relied on plasticization of lignin that contributed to "welding" cellulosic fibers during consolidation under pressure [8,32]. Moreover, the ability of fibers to "fuse" or weld together by lignin is an important factor during thermo-hydro-mechanical (THM) wood processing [33]. Therefore, the presence of lignin and its proper distribution in the cell wall can be a positive factor during production of wood-based composites and perhaps densified fuel pellets. These observations suggest that controlling the amount of lignin redistribution on particle surfaces, via thermal pretreatment (e.g., HWE), could provide a viable strategy to modify the material for downstream production of composite products and fuel pellets. Hence, understanding the influence of HWE factors on compositional changes to lignin in wood can be beneficial in adopting this pretreatment technology in a wood-based composites production plants for converting the plant into an integrated facility producing several products.

A number of works have been conducted to understand the mechanism(s) of lignin removal, relocation, reactions during HWE, impacts on biofuels production [4,6,7,18,22–25,28,29,34–41], and behavior of DCM extractable lignin during hot pressing of poplar wood [42]. Results showed that, for example, the molecular weight of residual lignin depends on the conditions (time, temperature, or equipment) of the HWE process [22,40,41]. It has been suggested that, in a related steam explosion process, manipulating the conditions of the process can modify the amount and properties of lignin [43,44]. Moreover, Sannigrahi et al. [28] mentioned that the amount of deposited lignin droplets on fiber surfaces increases as the severity of pretreatment progresses. These findings indicate that the conditions of the HWE process could impact lignin removal and properties. Similar conclusions have been drawn for other types of thermal treatments of wood such as torrefaction [31] and hot pressing [42].

Although previous studies report the effect of HWE on the composition of lignin in wood [45], there is limited information on the mechanism and quantity of the LLI deposition on the fiber surfaces during HWE, especially the inner surface of cells. The objective of this paper was to study the effect of the HWE conditions, measured by the severity factor (R_0), on the amount and properties of removable lignin-rich material (i.e., LLI) deposited on the wood particle surfaces after HWE. While other factors (e.g., amount of hemicelluloses, cell wall porosity, or cellulose degree of crystallinity) can affect both production and properties of biofuels, composites, and fuel pellets, this paper focuses on lignin.

2. Materials and methods

In the western US, densely stocked stands at risk for uncharacteristically severe wildfire are being thinned to improve forest health and reduce fire risk. This study sampled small-diameter (<25 cm at breast height) ponderosa pine (*Pinus ponderosa* Dougl. ex Laws.) 1986 plantation that was in need of fuel reduction treatment. The site is located in the Deschutes National Forest, Sisters Ranger District in central Oregon (elevation 1014 m, latitude 44.392803, longitude 121.674000). Trees were cut into 1.2-m bolts, banded and shrink wrapped in plastic for shipping to testing site. Average small-end diameter inside bark of the bolts was 9.1 cm. Bolts then were shipped to the testing site and chipped without removing the bark [46]. The resulting chips used as raw material in this study had a bark fraction of 14.0 ± 0.5%, as detailed in Ref. [11]. After drying at room conditions, the chips were ground using a Bliss Industries hammermill and the wood flour classified using standardized sieves to obtain particles with size ranging from 0.250 to 0.833 mm (60–20 mesh sieves, respectively). The selected wood flour was then dried (103 °C, 12 h) prior to extractives removal. Removal of extractives was conducted in order to avoid the effect of polyphenolic compounds and lignans present in extractives [47] when interpreting results of the composition of lignin after the HWE process [22]. Removal of extractives was performed following ASTM D1107–07 [48] with ethanol:toluene (2:1 vol/vol) as solvent, using a Soxhlet extraction apparatus.

2.1. Hot water extraction process

Dry, extracted wood flour was subjected to HWE using a 1-L Parr 4521 Bench top reactor controlled by a 4842 Parr controller and coupled with a water circulating cooling system. Approximately 20 g of pine flour were used for each run in the Parr reactor. E-pure water (Type I, ASTM D1193-06) was added to the container (a 1-L glass liner, Parr) to keep a water/wood relationship of 4:1 (mass/mass). The HWE process was conducted at different temperatures: 140, 160, 180, 200, 220, 240, 260, 280, 300, and 320 °C for 90 min, thus allowing us to test different levels of severity factor (R_o). The pH of the HWE extraction liquor was measured after cooling (i.e., at room temperature) using a pH meter (Mettler Toledo SevenEasy). In processes above 240 °C, part of the solids fused and stuck to the glass liner wall. Scraping was necessary to completely recover the solids. Afterward, the solid products were washed with tap water for neutralization, oven dried (103 °C, 24 h), and the corresponding yields of solids were recorded.

2.2. Severity factor (R_0) computation

The experimental data is presented in terms of the severity factor (R_o), determined as: $R_0 = t\ exp[(T_H - T_R)/14.75]$ [3], where t is reaction time (min), T_H is the hydrolysis temperature (°C), and T_R is a reference temperature (normally 100 °C). In processes where the pre-heating step is long in comparison with the isothermal step, degradation of wood constituents can take place even before reaching the setup temperature. In these situations, Borrega et al. [34,35] suggested adding a time-temperature correction factor (t_T). For computing the t_T, the E_a (activation energy) of ponderosa pine containing bark was determined as per ASTM D1641 [49]. The E_a of control pine was 175.2 kJ mol^{-1} and the E_a of HWE pine treated at 160 °C was 160.7 kJ mol^{-1}. Thus, 160 kJ mol^{-1} is an acceptable approximation of E_a in the range of temperatures tested. Lower values of E_a only slightly increased the t_T. The degradation rate was determined as the ratio of the fraction of mass degradation (loss) during the HWE process at a specific temperature to the isothermal HWE time. The results of the t_T were then added to the isothermal process time (i.e., 90 min).

2.3. Isolation/concentration of lignin liquid intermediate

The dried pine flour, following HWE process at different temperatures, was subsequently subjected to a process similar to that used for extractives removal, but using dichloromethane (DCM) as solvent as described in Ref. [31]. The intention of this step was to isolate/concentrate and quantify the abundance of materials that are DCM-soluble.

2.4. Characterization of products

Characterization of a) the control material (not subjected to HWE), b) HWE pine (at varying conditions), c) HWE solids after the DCM process, and d) DCM-soluble material isolated from HWE wood, was conducted following some of the procedures described in Ref. [31]. The next sections summarize these methods and additional procedures used.

2.4.1. Solids characterization

The characterization of the solids was carried out using pyrolysis gas chromatography/mass spectrometry (Py-GC/MS), and elemental analysis (carbon, hydrogen, nitrogen, sulfur–CHNS). Py-GC/MS tests were performed following the procedure described elsewhere [31]. Py-GC/MS for each sample was conducted in triplicate using a CDS pyroprobe 5000 series (CDS Analytical, Inc.) connected to a GC/MS system (6890N Network GC System with a 5975B inert XL MSD, from Agilent Technologies). The GC/MS system was equipped with an HP-5MS capillary column (30 m long x 0.25 mm diameter, nominal film thickness of 0.25 μm, from Agilent Technologies). For the tests, the CDS interface was set at 250 °C to avoid condensation of vapors [30]. Before each pyrolysis test the materials were weighed using a TGA balance (TGA/SDTA851e, Mettler Toledo) to obtain semi-quantitative results. The amount of material in each pyrolysis tests was 500–800 μg. The pyrolysis process started with inserting the sample probe in the oven of the DCS pyroprobe; after 0.2 min the temperature in the filament probe was increased to 500 °C (at a heating rate of 1073 K s^{-1}). This temperature was maintained for 1 min for pyrolysis. The GC inlet temperature was set at 250 °C. The temperature profile was set to maintain the initial temperature at 40 °C for 1 min, followed by a heating period at 279 K min^{-1} till 280 °C. The GC was maintained at the final temperature for 15 min. Helium was used as carrier gas (1 cm^3 min^{-1}) in split mode (50:1) at a total flow of 54 cm^3 min^{-1}. Identification of the compounds resulting from the pyrolysis was performed considering retention time, mass spectra, and comparison with database of the NIST/EPA/NIH Mass Spectral Library V. 2.0d (Fair Com Corp). Results were normalized by dividing the area of each representative peak (i.e., those with higher intensity) by the mass of the corresponding specimen [31].

Ash content in the initial and in the HWE materials was quantified following ASTM D1102–84 [50]. Elemental composition (CHN) was determined using a LECO® TruSpec CHN instrument [31]. For sulfur (S) analysis, a LECO® 628S S module was used. Approximately 0.1 g of dried material was fed into the 628S module after preparation following the procedure outlined in the Organic Application Note for Sulfur in Biomass and Biofuel (www.leco.com) and using LECO 528-203 crucibles. Results of ash content were used to calculate the oxygen content.

2.4.2. Characterization of DCM-soluble material

The DCM-soluble material was characterized for determining its composition, molecular weight, and behavior under heating conditions, using Py-GC/MS, electrospray ionization mass spectrometry (ESI-MS), and thermogravimetric analysis (TGA), respectively. Atomic force microscopy (AFM) and scanning electron microscopy (SEM) were also used to understand the ability of removed lignin-rich material (i.e., DCM-soluble material) to interact with cellulosic fibers. For Py-GC/MS, a process similar to that described previously for solids characterization was used, but the sticky nature of the samples forced us to use larger samples (0.6–0.8 mg, weighed using the TGA/SDTA 851e Mettler Toledo equipment).

2.4.2.1. ESI-MS and TGA. ESI-MS tests were carried out using an LCQ-Deca (Thermo Finnigan) instrument following the procedure decribed elsewhere [31]. TGA of DCM-soluble material was conducted to determine if there are differences in thermal stability and any pattern to thermal degradation of these materials. Due to limitations in material availability, only material isolated from HWE at 240, 260, 280, and 300 °C were evaluated. TGA (ASTM E1131-08) was performed in a TGA instrument (TA SDT Q600) under N_2 atmosphere (flow rate of 100 cm^3 min^{-1}) in the range of 35–500 °C at a heating rate of 283 K min^{-1}. Approximately 7 mg of sample was used for each test.

2.4.2.2. AFM and SEM. A small amount of DCM-soluble material isolated from HWE wood at two conditions, 200 and 220 °C, was blended with DCM and agitated, then drops of the solution (0.2 cm^3) were deposited on the surface of bond paper (X-9 Boise®). The paper containing the solution was dried under fume hood at room temperature (for less than 30 min, which was sufficient for complete evaporation of DCM) and a small piece (~6 × 6 mm) used for AFM analysis. A MultiMode™ Atomic Force Microscope (Veeco) controlled by a PicoForce™ Force Spectroscopy Control Module (Veeco) and Nanoscope V613r1 software were employed for the test. The samples were measured in tapping mode using a silicon probe force modulation cantilever (Veeco) hold in a multimode force modulation probe holder. First, images of 5 × 5 μm were recorded for obtaining an overview of the morphology of fibers covered by lignin. Then detailed images were acquired using a 2.5 × 2.5 μm sections at a scan rate of ~1 Hz. Image analysis was performed on the AFM scans (as captured) using the SPIP image analysis software (Image Metrology, version 6.1.1). No further image processing was performed. For SEM, a similar procedure was followed for sample preparation, using the DCM-soluble material removed from wood treated at 220, 240,260, 280, and 300 °C. An FEI Quanta 200F SEM was employed after gold sputtering of surfaces. For the test, the voltage was set to 20 kV.

3. Results and discussion

3.1. Influence of processing parameters on wood degradation

The extractives content of ponderosa pine (with bark) was 6.07 ± 0.22%. HWE of extracted ponderosa pine (i.e., pine subjected to ethanol/toluene extraction) at different temperatures resulted in wood degradation that varied from 18% to 50% (Fig. 1). The

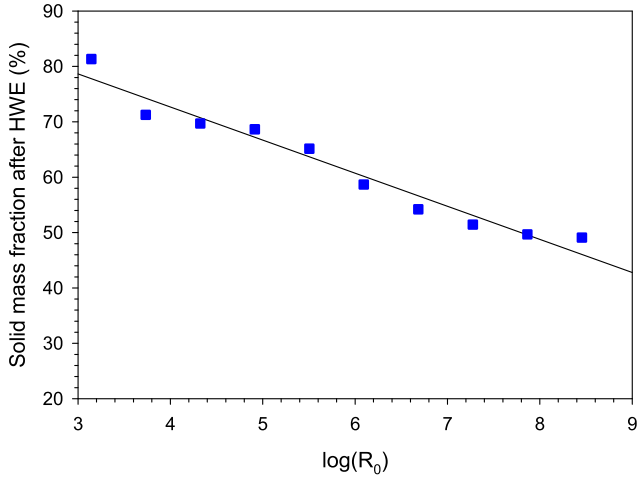

Fig. 1. Solids remaining after HWE at different levels of Severity Factor (R_0) (see Table 1 for logR_0 details). The stright line shows the tendency of the solids remainin after HWE.

percentage of the remaining solid after HWE is presented in Fig. 1, showing a negative linear relationship with increasing combined severity factor. The parameters used for computing *log(R_0)* are presented in Table 1. The time-temperature correction factor resulting from the pre-heating step varied from 2.5 min at 140 °C to 5 min at 320 °C and the pH varied from 3.4 to 3.0, respectively. As in torrefaction [31], an increase in color intensity was observed in HWE wood as the temperature of the process increased.

3.2. Properties of HWE material

3.2.1. Elemental composition of HWE material

The ash content and the elemental composition of the hot water extracted material changes with the pyrolysis conditions, as shown in Table 2. The ash content of the initial (control) material was 0.48%, which is close to previous results using the same material (i.e., 0.58 ± 0.07%) [11]. The relative ash content in HWE wood (Table 2) decreased slightly at temperatures up to ~220 °C. Under the conditions of our experiment, minimum percentages of ash content occur at approximately 180 °C and 90 min, which is in agreement with previous findings using pine wood chips (same material) instead of wood flour [11]. This result suggests that apparently the particle size has no effect on the yields of ash removal in HWE wood. Results of the elemental composition analysis (CHNS) of the control and materials after HWE at different conditions are also presented in Table 2. The sulfur content, as expected, was negligible (i.e., below detection limits). The percentage of C content in the material increased as the temperature of the HWE process increased. The H content slightly decreased and the N content remained approximately equal in the range of temperatures tested. The O content, as expected, decreased as the R_0 increased. Similar tendencies were observed during torrefaction of the same material at different temperatures [31]. A Van Kravelen diagram [51] was plotted using the elemental composition results. The diagram (Fig. 2) suggests that, as in torrefaction [31], dehydration is one of the main reactions occurring during HWE, confirming previous findings [52].

Table 2
Results of the elemental composition analysis. Ash fraction (third column) was used for elemental composition computations.

Material	Log(R_0)	Ash (%)	C (%)[a]	H (%)[a]	N (%)[a]	O (%)[a]
Control	–	0.48	50.80	6.59	0.19	42.42
140 °C[b]	3.1443	0.40	50.53	5.94	0.22	43.32
160 °C	3.7342	0.21	52.19	5.90	0.22	41.69
180 °C	4.3242	0.13	53.06	5.83	0.20	40.92
200 °C	4.9143	0.25	55.38	5.71	0.18	38.73
220 °C	5.5044	0.39	57.72	5.52	0.17	36.58
240 °C	6.0945	0.44	62.10	5.37	0.19	32.35
260 °C	6.6848	0.46	70.58	5.00	0.15	24.28
280 °C	7.2750	0.47	71.57	4.97	0.22	23.24
300 °C	7.8653	0.49	72.35	4.85	0.24	22.56
320 °C	8.4557	0.53	74.15	4.46	0.22	21.17

[a] Mass fractions on a moisture free basis. S content was neglibible.
[b] Referes to the HWE temperature.

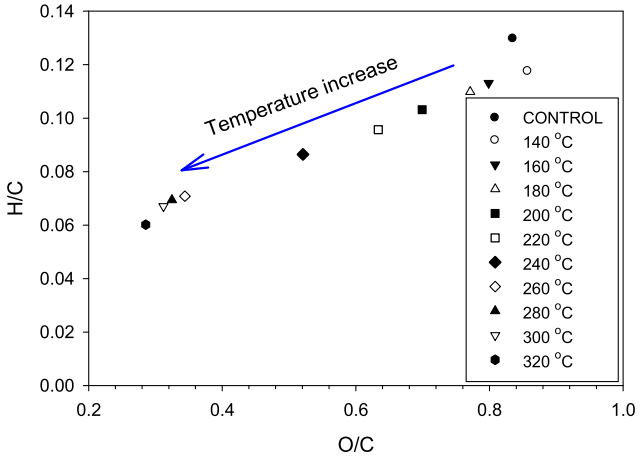

Fig. 2. Van Krevelen's diagram showing the variation of O/C and H/C as the severity of HWE changes.

3.2.2. Abundance of constituents in HWE wood

Typical normalized Py-GC/MS chromatograms of HWE wood at different conditions are presented in Fig. 3 and identification of labeled peaks is shown in Table 3. Py-GC/MS intended to investigate the trends of the abundance of the main wood constituents as the HWE severity increases. Since no pyrolysis products were detected after 24 min of retention time (i.e., the curve was almost flat), Fig. 3 shows the chromatogram until retention time of 24 min only. The Py-GC/MS chromatograms indicate that the intensity of peaks change with the severity of HWE. For example, the intensity of the peak corresponding to acetic acid (peak 3) decreases as the HWE severity increases. No acetic acid is apparently present in material after HWE at 180 °C and above. Levoglucosan (peak 22) abundance remains approximately constant in materials treated at up to 200 °C, after which its abundance seems to decrease. The abundance of phenols also appears to decrease but the actual trend is more difficult to ascertain. Thus, a graph of the tendency of the main pyrolysis products was prepared (Fig. 4). These results allow us to confirm the tendency of pyrolysis products, including phenols (derived from lignin pyrolysis [53]), to decrease as the severity of the HWE increases.

In order to indirectly quantify the presence of the main wood

Table 1
Conditions of the HWE process in terms of severity factor (R_0).

Set temperature (°C)[a]	Isothermal time (min)	Heating time (min)	Corrected time (min)	Log(R_0) (min)
140	90	40	92.6	3.1443
160	90	46	92.8	3.7342
180	90	52	93.1	4.3242
200	90	59	93.3	4.9143
220	90	64	93.6	5.5044
240	90	70	93.8	6.0945
260	90	76	94.1	6.6848
280	90	82	94.43	7.2750
300	90	89	94.8	7.8653
320	90	94	95.1	8.4557

[a] The actual temperature was not stable due to difficulty in stabilizing and controlling the set temperature in the Parr reactor. The temperatures ranged in the intervals 140 ± 2 °C, 160 ± 3 °C, 180 ± 3 °C, 200 ± 4 °C, 220 ± 4 °C, 240 ± 5 °C, 260 ± 5 °C, 280 ± 5 °C, 300 ± 5 °C, and 320 ± 5 °C.

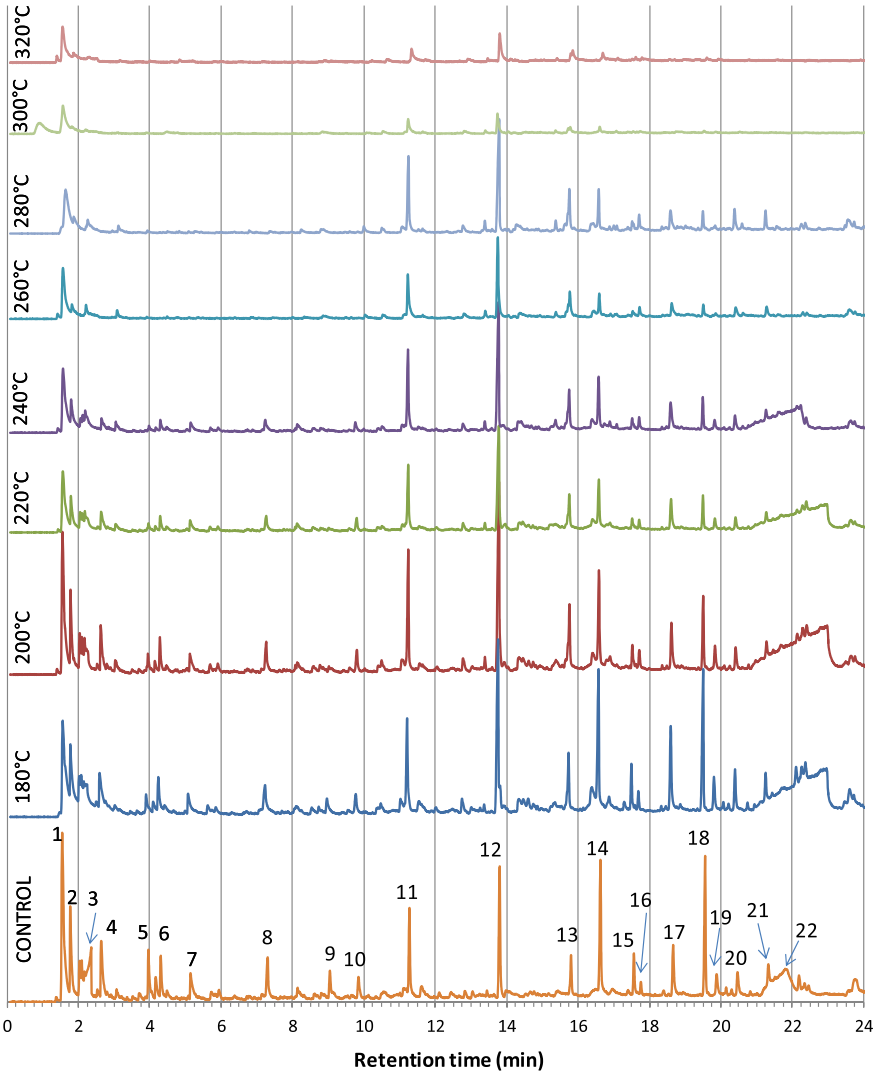

Fig. 3. Typical normalized chromatograms of HWE wood at different conditions (list of the related compunds is shown in Table 3) (normalization consisted on dividing peak area by the mass of the corresponding test sample).

constituents in the solid after HWE, the sum of the normalized areas of three main pyrolysis products (acetic acid, levoglucosan, and phenols) of each chromatogram were plotted (Fig. 5). It is confirmed that the abundance of acetic acid, which results from the deacetylation of hemicelluloses, decreases as the severity of HWE increases and that this compound is not detected in material treated at 180 °C ($logR_0 = 4.3242$) or higher. This result indicates that at these conditions most hemicelluloses were removed from wood. The amount of levoglucosan, typically derived from pyrolysis of cellulose, also decreases as the conditions of the process become more severe. No levoglucosan is seen at or above 260 °C ($logR_0 = 6.6848$). However, the presence of CO_2 in material treated at 320 °C suggests that some cellulose (which can degrade into CO_2), probably linked to lignin forming lignin carbohydrates complexes, is still present. Fig. 5 also suggests that the abundance of products of the pyrolysis of lignin (phenols) decreases as the pretreatment severity increases and that phenols are present even at high HWE temperatures. Although Py-GC/MS cannot accurately predict the abundance of the total lignin in the tested materials (in part because lignin pyrolysis can also produce CO_2 and because not all lignin pyrolysis products are detected with the equipment), Py-GC/MS helps to obtain a tendency of the presence of lignin in biomass as shown in previous works [54–57]. It is important to note, however, that the results show products of degradation of lignin independent of its location in the cell wall (i.e., it is not possible to detect if that lignin was inside the cell wall or on the surface of particles after migration during HWE).

3.3. Results of the characterization of the DCM-soluble material

3.3.1. Yields of DCM-soluble material

The DCM-soluble material showed an oily-like/gel-like morphology. This oily-like morphology of lignin-rich materials has been reported in previous works. For example, Tanahashi [58] mentioned the presence of a "lignin-like oily substance released from fibers" subjected to steam explosion. This type of morphology was also cited in Rezanowich and Goring [59], who studied the expansion of lignin sulfonate using a spherical microgel model; Goring [60], who mentioned that soluble lignins are spherical in shape; and Haas et al. [26], who used microscopy imaging for studying real time and post-reaction structure of biomass undergoing pyrolysis. The yield of this DCM-soluble oily-like substance, multiplied by the percentage of remaining solid after the HWE process (as seen in Fig. 1), are presented in Fig. 6. The differences in

Table 3
Identification of the main compounds found in the Py-GC/MS spectra of the pyrolysis of HWE wood (RT—retention time; m/z—mass/charge).

Peak#	RT	*m/z*	Compound	Name
1	1.64	44	CO_2	Carbon Dioxide
2	1.80	43	$C_5H_8O_2$	1-Propen-2-ol, acetate
3	2.38	43	$C_2H_4O_2$	Acetic acid
4	2.78	43	$C_3H_6O_2$	2-Propanone, 1-hydroxy-
5	3.99	43	$C_6H_{10}O_3$	2-Butanone, 1-(acetyloxy)-
6	4.43	43	$C_4H_6O_3$	Propanoic acid, 2-oxo-, methyl ester
7	5.14	96	$C_5H_4O_2$	Furfural
8	7.46	98	$C_5H_6O_2$	1,2-Cyclopentanedione
9	9.13	114	$C_8H_{17}NO$	Oxazolidine, 2,2-diethyl-3-methyl-
10	9.97	112	$C_6H_8O_2$	2-Cyclopenten-1-one, 2-hydroxy-3-methyl-
11	11.32	109	$C_7H_8O_2$	Phenol, 2-methoxy-
12	13.79	123	$C_8H_{10}O_2$	Phenol, 2-methoxy-4-methyl-
13	15.80	137	$C_9H_{12}O_2$	Phenol, 4-ethyl-2-methoxy-
14	16.62	135	$C_9H_{10}O_2$	2-Methoxy-4-vinylphenol
15	17.57	164	$C_{10}H_{12}O_2$	Eugenol
16	17.75	137	$C_{10}H_{14}O_2$	Phenol, 2-methoxy-4-propyl-
17	18.65	151	$C_8H_8O_3$	Vanillin
18	19.55	164	$C_{10}H_{12}O_2$	Phenol, 2-methoxy-4-(1-propenyl)-
19	19.88	137	$C_{10}H_{14}O_2$	Phenol, 2-methoxy-4-propyl-
20	20.47	151	$C_9H_{10}O_3$	Ethanone, 1-(4-hydroxy-3-methoxyphenyl)-
21	21.33	137	$C_{10}H_{12}O_3$	2-Propanone, 1-(4-hydroxy-3-methoxyphenyl)-
22	22.61	60	$C_6H_{10}O_5$	Levoglucosan
–	29.01	43	$C_{16}H_{32}O_2$	n-Hexadecanoic acid
–	31.86	55	$C_{18}H_{34}O_2$	Oleic acid
–	32.18	43	$C_{18}H_{36}O_2$	Octadecanoic acid

yields of DCM-soluble material between the control and materials treated at 140 and 320 °C were negligible. The yields of DCM-soluble products isolated from materials treated at 160 and 180 °C were very low, impeding for recovery in amounts that allow further analyses.

In a previous work [31], it was found that torrefaction of similar material also promotes the presence of a comparable DCM-soluble material on particles. However, the maximum yield of this substance in the HWE process (4.24 ± 0.17% at ~280 °C) is higher than the maximum yield observed in torrefied wood (~2.5% at ~300 °C). These results suggest that the presence of water could play an important role on the yields of removable DCM-soluble substance. At temperatures usually used for HWE, wood is subjected to hydrolysis reactions in the presence of hydronium ions generated by water autoionization, which act as catalysts [61], thus degrading wood to a greater extent than in the presence of nitrogen (in torrefaction) and possibly allowing lignin to migrate from the cell walls and middle lamella more easily. Results additionally suggest that it is possible to control the conditions of the HWE process to limit or increase the availability of DCM-soluble material. Thus, the

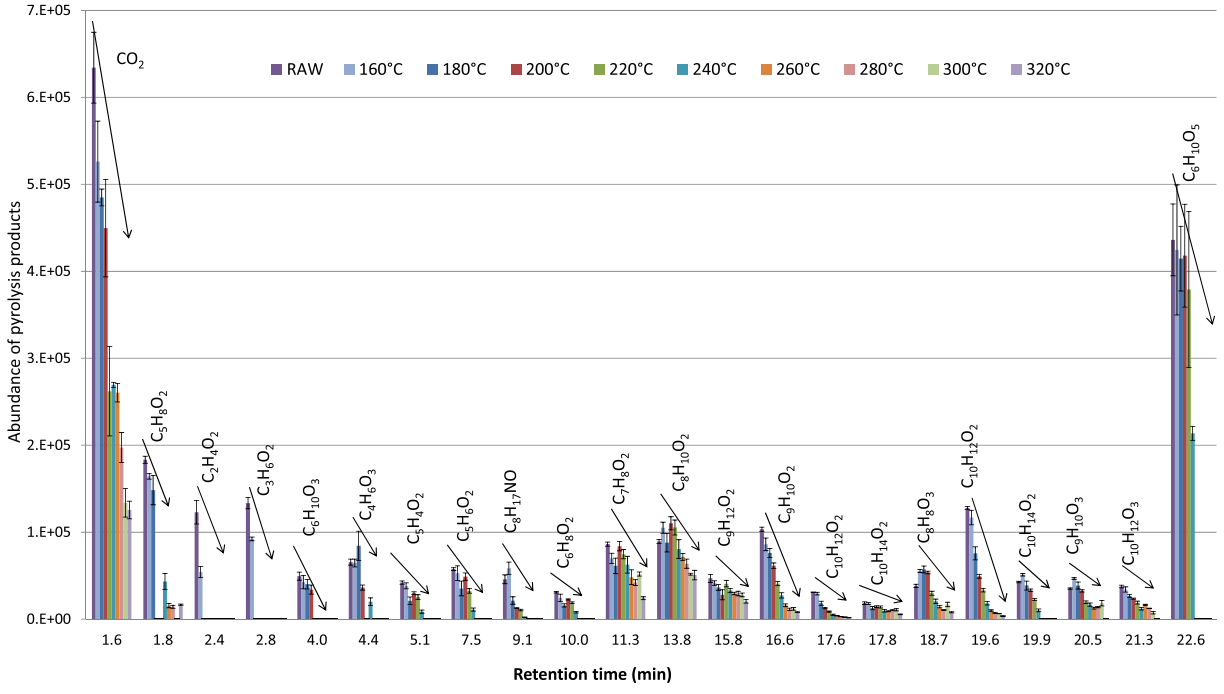

Fig. 4. Tendency of the abundance pyrolysis products of wood after HWE at different conditions.

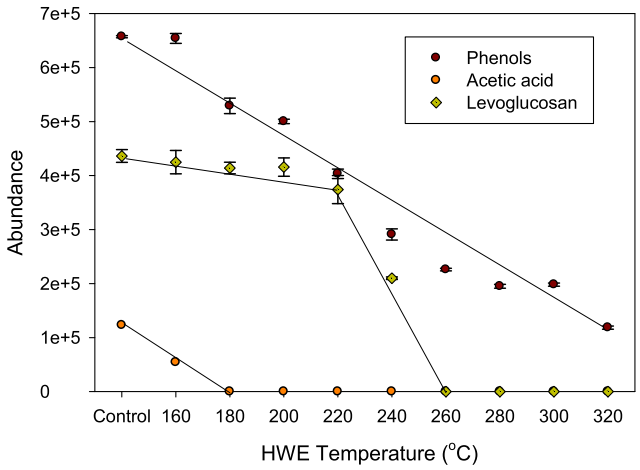

Fig. 5. Tendency of the abundance of the sum of products of the pyrolysis of HWE wood. The straight lines show the tendency of the abundance of products as the severity of HWE changes.

abundance of removable DCM-soluble material depends on the process conditions, as previously found in steam explosion process [44].

3.3.2. Composition of the DCM-soluble extract

Typical Py-GC/MS normalized chromatograms of the DCM-soluble material are presented in Fig. 7 and a list of the identified compounds is presented in Table 4. Py-GC/MS was performed to confirm that this DCM-soluble material was rich in lignin. Fig. 7 shows peaks of pyrolysis products up to retention time of 26 min as no pyrolysis products of interest were identified after this retention time, except those shown in Table 4 (mostly fatty acids). All samples (i.e., DCM-soluble material isolated from pine treated at different temperatures) present a common feature, which is the presence of peaks of phenols, with varying intensity. Since phenols are produced from the pyrolysis of lignin [53], these chromatograms indicate that the isolated DCM-soluble material is in fact lignin-rich. Comparison of the abundance of the main pyrolysis products (after normalization) (Fig. 8) in this lignin-rich material shows a peculiar tendency in the majority of phenols: the abundance increases up to certain temperature (around 240–260 °C) and decreases above this temperature (see blue arrows). Summing the area of all phenols at a specific temperature and then multiplying the sum by the yield of DCM-soluble material at the corresponding temperature, provides a pattern of the abundance of DCM-soluble lignin-rich material, and illustrated in Fig. 9.

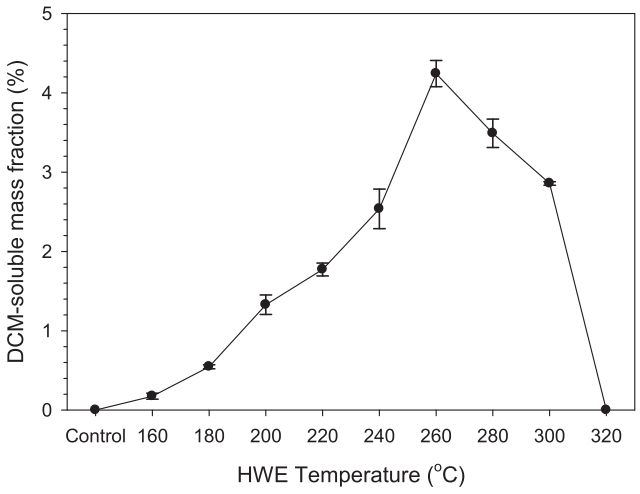

Fig. 6. Yields of DCM-soluble mass fraction (in dry feedstock basis).

An additional approach to confirm the nature of the DCM-soluble material was by comparing the abundance of phenols in the solid materials before and after the DCM process. Results (Fig. 10) show that, in general, the abundance of phenols in the pyrolysis products of materials pretreated at 220–280 °C, as expected, decreased after the DCM process.

3.3.3. Molecular weight of the DCM-soluble lignin

ESI-MS results showing both the number average molecular weight (M_n) and the weight average molecular weight (M_w) of DCM-soluble lignin-rich material isolated from HWE wood at different severity conditions are presented in Fig. 11. M_n and M_w are less than ~900 and 1200 g mol^{-1}, respectively, in all cases. These values show a decreasing tendency of molecular weight as the severity of the treatment increases. However, it appears that after a certain pretreatment condition (in our case in HWE at and above 260 °C) lignin is not able to continue depolymerizing and its molecular weight reaches a plateau. This result is in agreement with previous findings showing that, in the Alcell® process, the molecular weight of removable lignin decreased to a limiting size [62]. It is interesting to note that approximately similar values of molecular weight were observed in lignin-rich material removed from wood torrefied at temperatures ranging from 275 to 325 °C [31]. In addition, the molecular weight and polydispersity ($PD = M_w/M_n$) of lignin removed from HWE at 180 °C are similar to those of lignin removed from wood torrefied at 275 °C. Moreover, the PD is fairly constant throughout the entire range of HWE conditions tested and had a value less than 1.5 (Fig. 11), showing a relatively narrow dispersion of molecular weight.

Comparison of results with values reported in literature is difficult due to differences in lignin type, experimental conditions and techniques, and/or raw material. However, results in this work can be compared with HWE cellulolytic enzyme lignin (CEL), lignin isolated with solvents from steam-exploded wood, and organosolv lignin. The values of molecular weight of HWE CEL are slightly higher (i.e., $M_n = 1500–3000$ g mol^{-1}, $M_w = 3200–13500$ g mol^{-1}) [40,41]. Organosolv lignin obtained from wood (i.e., $M_n = 4690$ g mol^{-1}, $M_w = 7060$ g mol^{-1}) [63] showed molecular weight values higher that those obtained in this work. However, the technique used by the author was different (gel permeation chromatography), thus making difficult comparison of results. Findings in this work and those in previous research [22,40,41] suggest that the more severe the pretreatment, the lower the values of M_w of extractable soluble lignin. However, Hergert et al. [62] showed that in the Alcell® process, extending the cooking time does not further reduce molecular weight of lignin, but temperature increase and wood species do impact molecular weight. The reduction of lignin molecular weight can result from the cleavage of some inter-unit bonds, mainly β-O-4 ether bonds [43,62–65], which are the most abundant type of linkages in lignin [66–69]. Since values of PD approaching two are associated with reduction of molecular weight by random scission [19], results suggest a random cleavage of lignin molecules during depolymerization. PD > 1 is characteristic of branched polymers [19], which is the case with lignin.

3.3.4. AFM and SEM results

AFM has been used to visualize cellulosic fibers after lignin precipitation [70–72] or enzymatic digestion [73]. In this work, AFM was used for investigating how lignin-rich material (isolated with DCM) interacts with cellulosic fibers. The morphology of

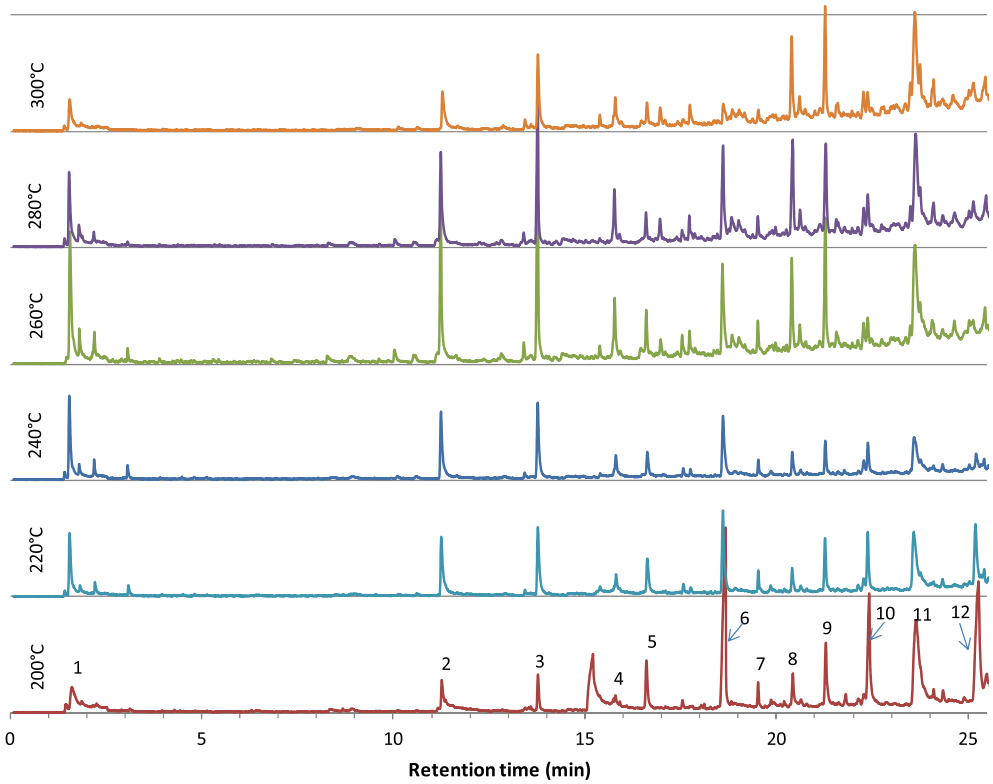

Fig. 7. Typical Py-GC/MS chromatograms of DCM-soluble lignin (blue arrows are used to identify some peaks).

lignin-rich material deposited on the surface of bond paper is observed in Fig. 12. Only results of material removed from HWE at 200 °C are shown because a similar morphology was visible in materials isolated from HWE wood at the other HWE conditions. Both AFM and SEM micrographs suggest that this lignin-rich material tends to adhere to the surface of the cellulosic fibers in the bond paper and form agglomerates of different shapes and sizes, with preference to form granular blobs (with prevalence of semi-spherical shape) (Fig. 12 c, d, e, f). Lignin's tendency to adhere and agglomerate on cellulosic fibers has been mentioned previously [70], which may result from the opposite charges between the surface and the lignin droplets [19,59,70]. Spherical shape has been previously observed in various types of lignin (e.g. sodium lignosulphonate, alkali lignin, dioxane lignin) and identified as a natural form of lignin agglomeration [59,60,74]. Tendency of lignin molecules (i.e., oligomers) to agglomerate and form globules has also been hypothesized as a step in the formation of pyrolytic lignin [75]. Thus, it appears that the DCM-soluble lignin-rich material shows a similar preference to form droplets and/or agglomerates of droplets. Moreover, this material is able to adhere to cellulosic fibers, explaining in part the adhesion of lignocellulosic fibers during consolidation of wood composites.

3.3.5. *Thermogravimetric characteristics of the DCM-soluble material*

Results of the thermogravimetry studies of the DCM-soluble lignin (isolated from HWE wood at temperatures from 240 to 300 °C) are presented in Fig. 13. Increasing the severity of the HWE process produces an extractable lignin with progressive decrease of thermal stability (Fig. 13a, see arrow). Lignin removed via HWE at both 240 and 260 °C (herein referred to as group A) behave in a similar fashion, while lignin removed via HWE at 280 and 300 °C (group B) begin degrading at a lower temperature. The DTG curves (Fig. 13b), on the other hand, show that the maximum rate of degradation occurs at approximately 210 °C and 230 °C, for groups A and B, respectively. A small peak visible at ~100 °C could result

Table 4
Main compounds identified in the Py-GC/MS chromatogram of Fig. 8, corresponding to the pyrolysis of DCM-soluble material (RT—retention time).

Peak#	RT	*m/z*	Compound	Name
1	1.57	44	CO_2	Carbon Dioxide
2	11.26	109	$C_7H_8O_2$	Phenol, 2-methoxy-
3	13.79	123	$C_8H_{10}O$	Phenol, 2-methoxy-4-methyl-
4	15.80	137	$C_9H_{12}O_2$	Phenol, 4-ethyl-2-methoxy-
5	16.65	135	$C_9H_{10}O_2$	2-Methoxy-4-vinylphenol
6	18.63	151	$C_{20}H_{28}O_{13}$	Vanillin
7	19.55	164	$C_{10}H_{12}O_2$	Phenol, 2-methoxy-4-(1-propenyl)-, (E)-
8	20.40	151	$C_9H_{10}O_3$	Ethanone, 1-(4-hydroxy-3-methoxyphenyl)-
9	21.32	137	$C_{10}H_{12}O_3$	2-Propanone, 1-(4-hydroxy-3-methoxyphenyl)-
10	22.43	151	$C_9H_{11}NO_3$	α-Amino-3'-hydroxy-4'-methoxyacetophenone
11	23.75	137	$C_9H_{10}O_4$	Acetic acid, (4-hydroxy-3-methoxyphenyl)-
12	25.23	178	$C_{10}H_{10}O_3$	.(2E)-3-(4-Hydroxy-2-methoxyphenyl)-2-propenal#

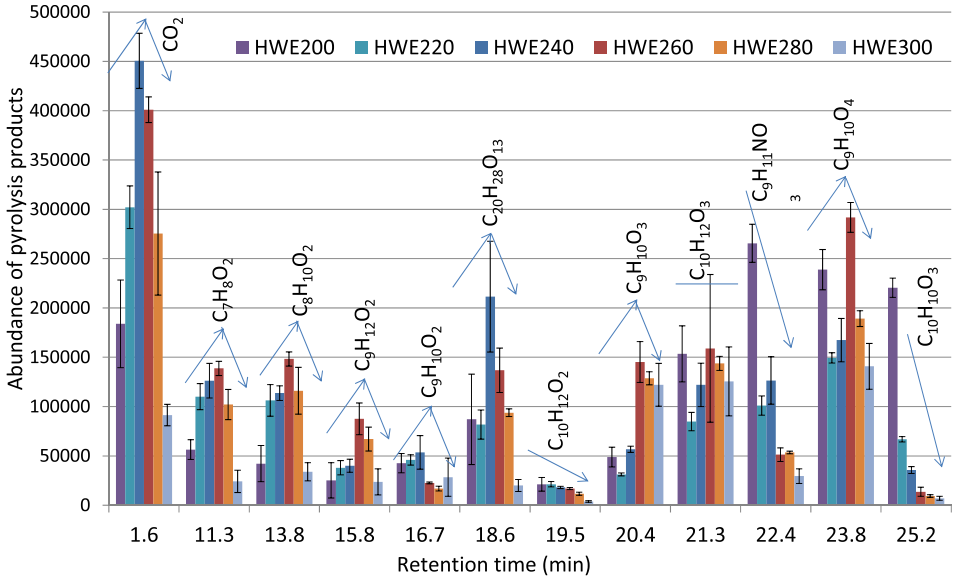

Fig. 8. Trend of the abundance (peak area divided by mass pyrolyzed) of pyrolysis products of the DCM-soluble material isolated from HWE pine at different temperatures. The blue arrows show the tendency of the abundance.

from the evaporation of moisture and probably some solvent present in the samples. A secondary peak is observed in the range 320–380 °C, which could be related with the presence of fractions of higher molecular weight compounds.

The reduction of the thermal stability of isolated lignin-rich material as the severity of the HWE process increases is apparently correlated with its molecular weight, as previously reported by Yoshida et al. [76] and Sun et al. [77]. In most polymers there is a direct relationship between molecular weight and glass transition temperature (T_g) [78], which has been verified in the case of lignin [19,79–81].

TGA results also show that the remaining mass (non-volatile residue) after the TGA process decreases as the HWE process temperature increases (Fig. 13a). Specifically, at the end of the TGA process (at 500 °C), the residual mass varies from 34% (for lignin isolated from HWE wood at 240 °C) to 19% (for lignin isolated from HWE wood at 300 °C). This result is expetected as the molecular weight of lignin decreased with increasing HWE temperature. Visual inspection of the residual material showed it to be a char-like material firmly adhered to the wall of the crucible used for TGA.

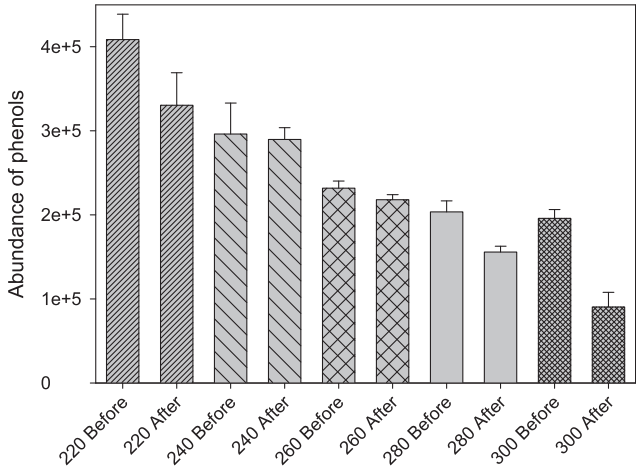

Fig. 10. Comparison of the abundance of phenols derived from the pyrolysis of the solid fraction before and after the DCM process. The numbers on the x-axis correspond to the temperature at which HWE was conducted.

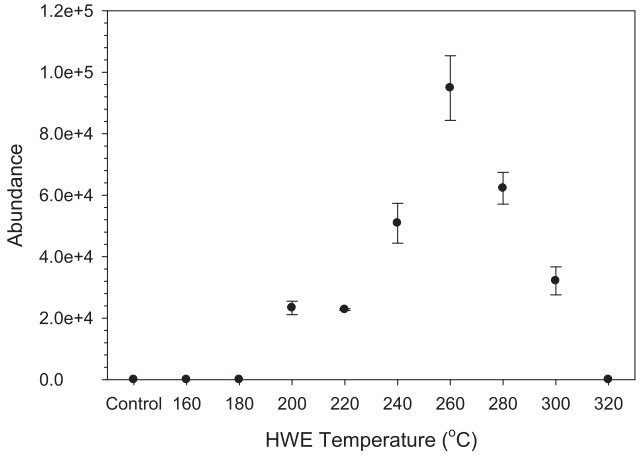

Fig. 9. Abundance of phenolic products of the pyrolysis of the DCM-soluble lignin isolated from HWE wood at different HWE conditions.

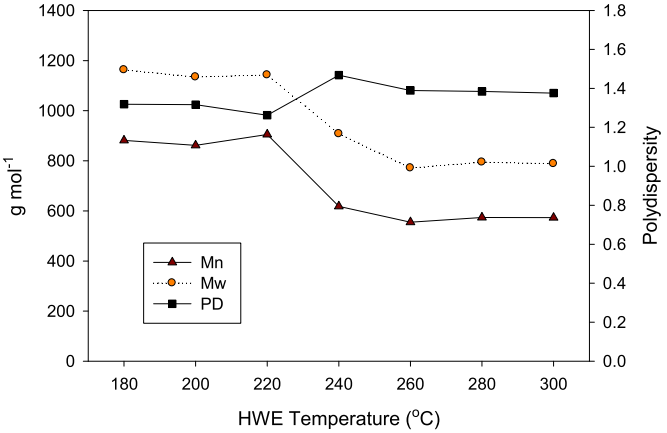

Fig. 11. Molecular weight and polydispersity (PD) of DCM-soluble lignin removed from HWE wood at different temperatures.

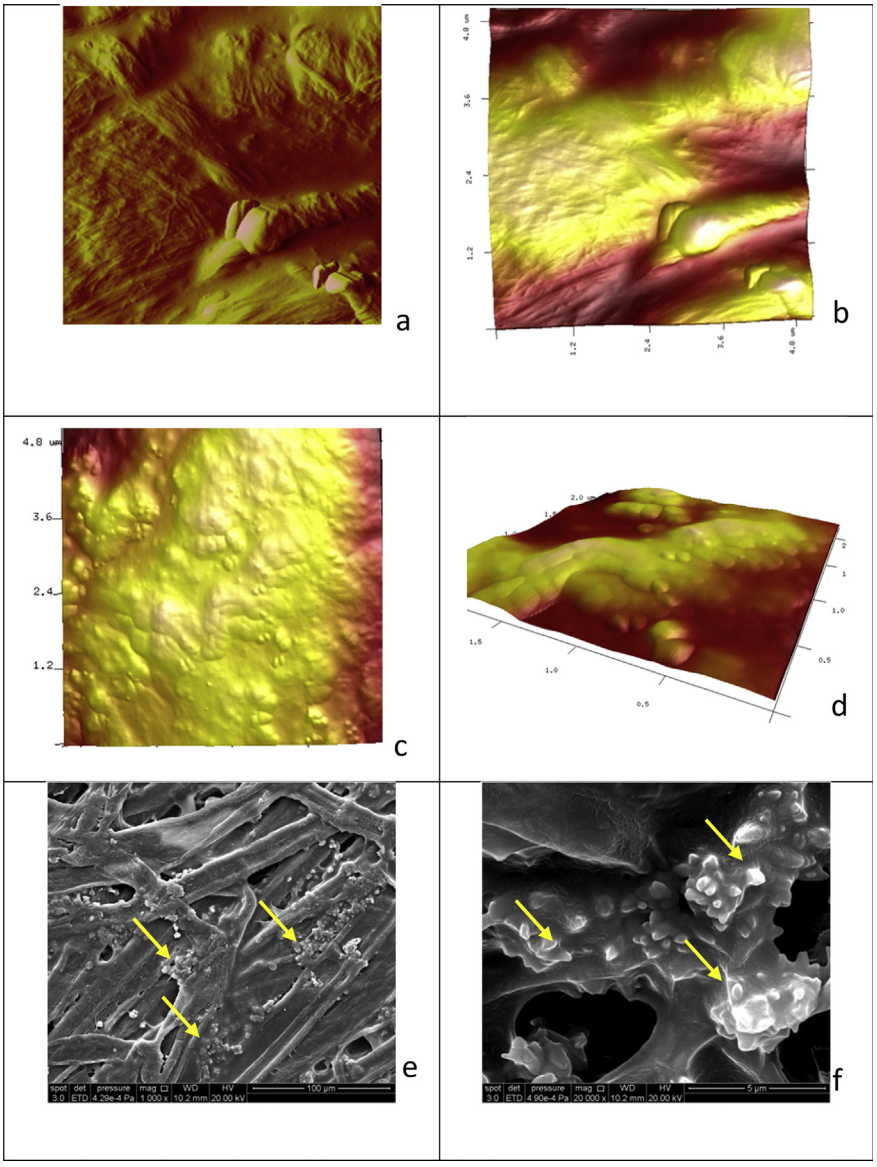

Fig. 12. 2-Dimensional AFM amplitude (a) and 3-Dimensional AFM height (b) pictures showing bond paper with some sporadic agglomerates of lignin-rich material; 3D AFM height pictures (c and d) of cellulosic fibers covered by abundant lignin aggregates (at two levels of magnification). Similar results (see arrows) were obtained by SEM analysis (e, f) (at two levels of magnification).

This char-like morphology is expected from lignin degradation via pyrolysis or hydrothermal processes [38,82–84]. In general, the findings of this research suggest that it is possible to control the temperature of the HWE process to alter the composition, structure, and abundance of LLI that can further be isolated from HWE wood using polar solvents such as DCM.

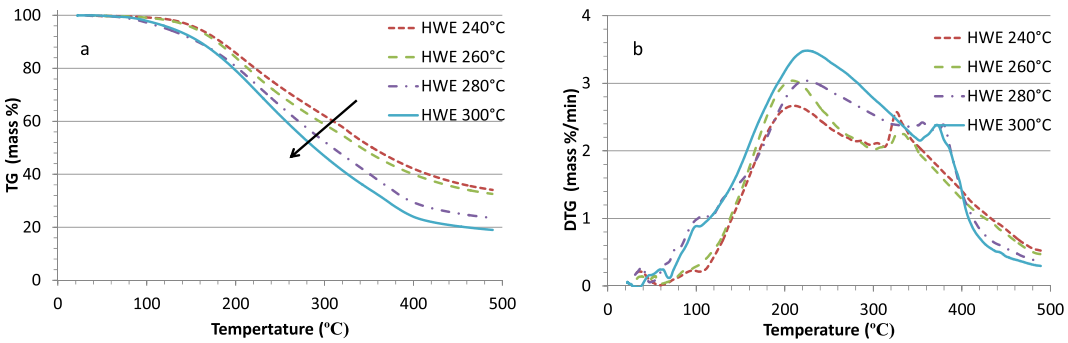

Fig. 13. TGA and DTG curves of DCM-soluble lignin removed from HWE pine.

4. Conclusion

HWE at varying conditions was conducted using ponderosa pine to study the behavior of lignin. This work found that the conditions of the thermal operations play an important role on the abundance, structure, and thermal stability of lignin-rich material that can be isolated from wood particles after HWE. Characterization of both the solid material after the DCM process and the lignin-rich material isolated with DCM suggest that during HWE lignin can migrate from the cell walls to the surface of fiber where it is deposited in part. This lignin-rich material presents properties that depend on the conditions of the operation. Since lignin on the surface of particles can play an important role in downstream processes, controlling its abundance to some extent could benefit wood-derived products properties.

Acknowledgment

The support of the USDA Forest Service Research and Development Woody Biomass, Bioenergy, and Bioproducts 2009 Grant Program (Agreement No. 09-JV-11261975-028) is acknowledged. M.R.Pelaez-Samaniego acknowledges the Fulbright Faculty Development Program Scholarship. The authors acknowledge Dr. Armando McDonald (University of Idaho) and the Franceschi Microscopy Center (Washington State University) for providing assistance on conducting the ESI/MS and SEM tests, respectively.

References

[1] S.Y. Ding, Y.S. Liu, Y.N. Zeng, M.E. Himmel, J.O. Baker, E.A. Bayer, How does plant cell wall nanoscale architecture correlate with enzymatic digestibility? Science 338 (6110) (2012) 1055–1060.
[2] Y. Zeng, S. Zhao, S. Yang, S.-Y. Ding, Lignin plays a negative role in the biochemical process for producing lignocellulosic biofuels, Curr. Opin. Biotech. 27 (2014) 38–45.
[3] H.L. Chum, D.K. Johnson, S.K. Black, R.P. Overend, Organosolv pretreatment for enzymatic hydrolysis of poplars. 2. Catalyst effects and the combined severity parameter, Ind. Eng. Chem. Res. 29 (2) (1990) 156–162.
[4] C.I. Ishizawa, T. Jeoh, W.S. Adney, M.H. Himmel, D.K. Johnson, M.F. Davis, Can delignification decrease cellulose digestibility in acid pretreated corn stover? Cellulose 16 (4) (2009) 677–686.
[5] B. Yang, Z. Dai, S.Y. Ding, C.E. Wyman, Enzymatic hydrolysis of cellulosic biomass, Biofuels 2 (4) (2011) 421–450.
[6] J.D. DeMartini, S. Pattathil, J.S. Miller, S. Li, M.G. Hahn, C.E. Wyman, Investigating plant cell wall components that affect biomass recalcitrance in poplar and switchgrass, Energy Environ. Sci. 6 (2013) 898–908.
[7] M.H. Studer, J.D. DeMartini, M.F. Davis, R.W. Sykes, B. Davison, M. Keller, et al., Lignin content in natural populus variants affects sugar release, PNAS 108 (15) (2011) 6300–6305.
[8] Mason WH, Inventor: Mason Fibre Co., assignee. Integral insulating board with hard welded surfaces. United States patent US 1663506, 1928 Mar 20.
[9] M.D. Shaw, C. Karunakaran, L.G. Tabil, Physicochemical characteristics of densified untreated and steam exploded poplar wood and wheat straw grinds, Biosyst. Eng. 103 (2009) 198–207.
[10] P.S. Lam, S. Sokhansanj, X. Bi, C.J. Lim, S. Melin, Energy input and quality of pellets made from steam-exploded douglas fir (*Pseudotsuga menziesii*), Energy Fuels 25 (2011) 1521–1528.
[11] T.L. Chaffee, Potential for Enhanced Properties of Wood Products by Hot Water Extraction of Low Value, Undebarked Ponderosa Pine (Master's thesis), State University of New York, Syracuse, 2011.
[12] T. Runge, P. Wipperfurth, C. Zhang, Improving biomass combustion quality using a liquid hot water treatment, Biofuels 4 (2013) 73–83.
[13] M.R. Pelaez-Samaniego, V. Yadama, M. Garcia-Perez, E. Lowell, R. Zhu, K. Englund, Interrelationship between lignin-rich dichloromethane extracts of hot water-treated wood fibers and high-density polyethylene (HDPE) in wood plastic composite (WPC) production, Holzforschung (2015), http://dx.doi.org/10.1515/hf-2014-0309.
[14] M.R. Pelaez-Samaniego, V. Yadama, E. Lowell, R. Espinoza-Herrera, A review of wood thermal pretreatments to improve wood composite properties, Wood Sci. Technol. 47 (2013) 1285–1319.
[15] M.R. Pelaez-Samaniego, V. Yadama, T. Garcia-Perez, E. Lowell, T. Amidon, Effect of hot water extraction on particleboard produced from hardwood and softwood, Holzforschung (2014), http://dx.doi.org/10.1515/hf-2013-0150.
[16] T.E. Amidon, C.D. Wood, A.M. Shupe, Y. Wang, M. Graves, S. Liu, Biorefinery: conversion of woody biomass to chemicals, energy and materials, J. Biobased Mater. Bio 2 (2008) 100–120.
[17] R.L. Johnson, S.-S. Liaw, M. Garcia-Perez, S. Ha, S.-S. Lin, A. McDonald, S. Chen, Pyrolysis gas chromatography studies to evaluate high-temperature aqueous pretreatment as a way to modify the composition of bio-oil from fast pyrolysis of wheat straw, Energy Fuels 23 (12) (2009) 6242–6252.
[18] J.Q. Bond, A.A. Upadhye, H. Olcay, G.A. Tompsett, J. Jae, R. Xing, et al., Production of renewable jet fuel range alkanes and commodity chemicals from integrated catalytic processing of biomass, Energy Env. Sci. (2014), http://dx.doi.org/10.1039/c3ee43846e.
[19] D.A.I. Goring, Polymer properties of lignin and lignin derivatives, in: K.V. Sarkanen, C.H. Ludwig (Eds.), Lignins. Occurrence, Formation, Structure and Reactions, Wiley-Interscience, New York, 1971, ISBN 0-471-75422-6, pp. 695–798.
[20] L. Salmen, Temperature and Water Induced Softening Behaviour of Wood Fiber Based Materials (PhD dissertation), The Royal Institute of Technology, Stockholm, 1982.
[21] G.M. Irvine, The glass transition of lignin and hemicellulose and their measurement by differential thermal analysis, Tappi J. 67 (5) (1984) 118–121.
[22] M.G.S. Chua, M. Wayman, Characterization of autohydrolysis aspen (*P. tremuloides*) lignins. Part 1. Composition and molecular weight distribution of extracted autohydrolysis lignin, Can. J. Chem. 57 (1979) 1141–1149.
[23] J. Li, G. Henriksson, G. Gellerstedt, Lignin depolymerization/repolymerization and its critical role for delignification of aspen wood by steam explosion, Bioresour. Technol. 98 (2007) 3061–3068.
[24] B.S. Donohoe, S.R. Decker, M.P. Tucker, M.E. Himmel, T.B. Vinzant, Visualizing lignin coalescence and migration through maize cell walls following thermochemical pretreatment, Biotechnol. Bioeng. 101 (5) (2008) 913–925.
[25] M.J. Selig, S. Viamajala, S.R. Decker, M.P. Tucker, M.E. Himmel, T.B. Vinzant, Deposition of lignin droplets produced during dilute acid pretreatment of maize stems retards enzymatic hydrolysis of cellulose, Biotechnol. Prog. 23 (2007) 1333–1339.
[26] T.J. Haas, M.R. Nimlos, B.S. Donohoe, Real-time and post-reaction microscopic structural analysis of biomass undergoing pyrolysis, Energy Fuels 23 (2009) 3810–3817.
[27] R.J.M. Westerhof, D.W.F. Brilman, M. Garcia-Perez, Z. Wang, S.R.G. Oudenhoven, S.R.A. Kersten, Stepwise fast pyrolysis of pine wood, Energy Fuels 26 (2012) 7263–7273.
[28] P. Sannigrahi, D.H. Kim, S. Jung, A. Ragauskas, Pseudo-lignin and pretreatment chemistry, Energy Env. Sci. 4 (4) (2011) 1306–1310.
[29] D. Min, Q. Li, V. Chiang, H. Jameel, H. Chang, L. Lucia, The influence of lignin–carbohydrate complexes on the cellulase-mediated saccharification I: Transgenic black cottonwood (western balsam poplar, California poplar) *P. trichocarpa* including the xylan down-regulated and the lignin down-regulated lines, Fuel 119 (2014) 207–213.
[30] S. Zhou, M. Garcia-Perez, B. Pecha, A.G. McDonald, R.J.M. Westerhof, Effect of particle size on the composition of lignin derived oligomers obtained by fast pyrolysis of beech wood, Fuel 125 (2014) 15–19.
[31] M.R. Pelaez-Samaniego, V. Yadama, M. Garcia-Perez, E. Lowell, A.G. McDonald, Effect of temperature during wood torrefaction on the formation of lignin liquid intermediates, J. Anal. Appl. Pyrol 109 (2014) 222–233.
[32] E.L. Back, The bonding mechanism in hardboard manufacture, Holzforschung 41 (1987) 247–258.
[33] P. Navi, D. Sandberg, Thermo-hydro-mechanical Wood Processing, first ed., EPFL Press, Boca Raton, FL, 2012.
[34] M. Borrega, K. Nieminen, H. Sixta, Degradation kinetics of the main carbohydrates in birch wood during hot water extraction in a batch reactor at elevated temperatures, Bioresour. Technol. 102 (2011) 10724–10732.
[35] M. Borrega, K. Nieminen, H. Sixta, Effects of hot water extraction in a batch reactor on the delignification of birch wood, BioResources 6 (2) (2011) 1890–1903.
[36] J.D. DeMartini, S. Pattathil, U. Avci, K. Szekalski, K. Mazumder, M.G. Hahn, et al., Application of monoclonal antibodies to investigate plant cell wall deconstruction for biofuels production, Energy Environ. Sci. 4 (2011) 4332–4339.
[37] L. Kumar, V. Arantes, R. Chandra, J. Saddler, The lignin present in steam pretreated softwood binds enzymes and limits cellulose accessibility, Bioresour. Technol. 103 (2012) 201–208.
[38] J. Hu, D. Shen, S. Wu, H. Zhang, R. Xiao, Effect of temperature on structure evolution in char from hydrothermal degradation of lignin, J. Anal. Appl. Pyrol 106 (2014) 118–124.
[39] D.D. Laskar, J. Zeng, L. Yan, S. Chen, B. Yang, Characterization of lignin derived from water-only flowthroughpretreatment of *Miscanthus*, Ind. Crops Prod. 50 (2013) 391–399.
[40] H.L. Trajano, N.L. Engle, M. Foston, A.J. Ragauskas, T.J. Tschaplinski, C.E. Wyman, The fate of lignin during hydrothermal pretreatment, Biotechnol. Biofuels 6 (2013) 110–126.
[41] R. Samuel, S. Cao, B.K. Das, F. Hu, Y. Pu, A.J. Ragauskas, Investigation of the fate of poplar lignin during autohydrolysis pretreatment to understand the biomass recalcitrance, RSC Adv. 3 (2013) 5305–5309.
[42] N.B. Osman, A.G. McDonald, M.-P.G. Laborie, Analysis of DCM extractable components from hot-pressed hybrid poplar, Holzforschung 66 (8) (2012) 927–934.
[43] R.H. Marchessault, S. Coulombe, H. Morikawa, D. Robert, Characterization of aspen exploded wood lignin, Can. J. Chem. 60 (1983) 2372–2382.
[44] DeLong EA, Ritchie GS, Inventors. Method for fractionation of lignins from steam exploded lignocellulosics to provide fractions with different properties. United States patent US 4966650, 1990 Oct 30.

[45] R. Martin-Sampedro, E.A. Capanema, I. Hoeger, J.C. Villar, O.J. Rojas, Lignin changes after steam explosion and laccase-mediator treatment of eucalyptus wood chips, J. Agric. Food Chem. 59 (2011) 8761–8769.
[46] M.R. Pelaez-Samaniego, V. Yadama, E. Lowell, T. Amidon, T.L. Chaffee, Hot water extracted wood fiber for production of wood plastic composites (WPCs), Holzforschung 67 (2) (2012) 193–200.
[47] E. Sjöström, Wood chemistry. Fundamentals and Applications, Academic Press, Orlando, FL, 1981.
[48] ASTM, Standard Test Method for Ethanol-toluene Solubility of Wood D1107-96, American Society for Testing and Materials, West Conshohocken, PA (USA), 2013.
[49] ASTM, Standard Test Method for Decomposition Kinetics by Thermogravimetry E1641-04, American Society for Testing and Materials, West Conshohocken, PA (USA), 2004.
[50] ASTM, Standard Test Method for Ash in Wood D1102-84, American Society for Testing and Materials, West Conshohocken, PA (USA), 2013.
[51] D.W. Van Krevelen, Coal: Typology, Chemistry, Physics, Constitution, Third ed., Elsevier Science Publishers B.V, Amsterdam, 1993.
[52] N. Kobayashi, N. Okada, A. Hirakawa, T. Sato, J. Kobayashi, S. Hatano, et al., Characteristics of solid residues obtained from hot-compressed-water treatment of woody biomass, Ind. Eng. Chem. Res. 48 (2009) 373–379.
[53] M. Zhang, F.L.P. Resende, A. Moutsoglou, Catalytic fast pyrolysis of aspen lignin via Py-GC/MS, Fuel 116 (2014) 358–369.
[54] J. Rodrigues, J. Graça, H. Pereira, Influence of tree eccentric growth on syringyl:guaiacyl ratio in *Eucalyptus globules* wood lignin assessed by analytical pyrolysis, J. Anal. Appl. Pyrolysis 58–59 (2001) 481–489.
[55] A. Alves, M. Schwanninger, H. Pereira, J. Rodrigues, Analytical pyrolysis as a direct method to determine the lignin content in wood. Part 1: comparison of pyrolysis lignin with Klason lignin, J. Anal. App. Pyrolysis 76 (2006) 209–213.
[56] A. Alves, J. Rodrigues, R. Wimmer, M. Schwanninger, Analytical pyrolysis as a direct method to determine the lignin content in wood Part 2: Evaluation of the common model and the influence of compression wood, J. Anal. Appl. Pyrolysis 81 (2008) 167–172.
[57] R. Fahmi, A.V. Bridgwater, S.C. Thain, I.S. Donnison, P.M. Morris, N. Yates, Prediction of Klason lignin and lignin thermal degradation products by Py–GC/MS in a collection of *Lolium* and *Festuca* grasses, J. Anal. Appl. Pyrolysis 80 (2007) 16–23.
[58] M. Tanahashi, Characterization and degradation mechanisms of wood components by steam explosion and utilization of exploded wood, Wood Res. 77 (1990) 49–117.
[59] A. Rezanowich, W.Q. Yean, D.A.I. Goring, High resolution electron microscopy of sodium lignin sulfonate, Appl. Polym. Sci. 81 (1964) 1801–1812.
[60] D.A.I. Goring, Thermal softening of lignin, hemicellulose and cellulose, Pulp Pap. Mag. Can. 64 (12) (1963) 517527.
[61] G. Garrote, H. Dominguez, J.C. Parajo, Hydrothermal processing of lignocellulosic materials, Holz Roh Werkst 57 (1990) 191–202.
[62] H.L. Hergert, G.C. Goyal, J.H. Lora, Limiting molecular weight of lignin from autocatalyzed organozolv pulping of hardwood, in: W.G. Glasser, R.A. Northey, T.P. Schultz (Eds.), Lignin: Historical, Biological, and Materials Perspectives, ACS Symposium Series, 742, American Chemical Society, Washington, DC, 1999.
[63] R. El Hage, N. Brosse, L. Chrusciel, C. Sanchez, P. Sannigrahi, Ragauskas. Characterization of milled wood lignin and ethanol organosolv lignin from miscanthus, Polym. Degrad. Stabil. 94 (2009) 1632–1638.
[64] K. Lundquist, Low-molecular weight lignin hydrolysis products, Appl. Polym. Symp. 28 (1976) 1393–1407.
[65] D. Dimmel, D. Gellerstedt, Chemistry of alkaline pulping, in: C. Heitner, D.R. Cimmel, J.A. Schmidt (Eds.), Lignin and Lignans. Advances in Chemistry, CRC Press, Taylor & Francis Group, Boca Raton, 2010.
[66] D. Fengel, G. Wegener, Wood. Chemistry, Ultrastructure, Reactions, Walter de Gruyter, Berlin, 1984.
[67] P.M. Froass, A.J. Ragauskas, J. Jiang, Chemical structure of residual lignin from Kraft pulp, J. Wood Chem. Techn 16 (4) (1996) 347–365.
[68] J.L. McCarthy, A. Islam, Lignin chemistry, technology, and utilization: A brief history, in: W.G. Glasser, R.A. Northey, T.P. Schultz (Eds.), Lignin: Historical, Biological, and Materials Perspectives, ACS Symposium Series, 742, American Chemical Society, Washington, DC, 2000.
[69] J. Ralph, K. Lundquist, G. Brunow, L. Lu, H. Kim, P.F. Schatz, et al., Lignins: Natural polymers from oxidative coupling of 4-hydroxyphenylpropanoids, Phytochem. Rev. 3 (2004) 29–60.
[70] N. Maximova, M. Österberg, K. Koljonen, P. Stenius, Lignin adsorption on cellulose fibre surfaces: effect on surface chemistry,surface morphology and paper strength, Cellulose 8 (2001) 113–125.
[71] E. Gilli, F. Schmied, S. Diebald, A.T. Horvath, C. Teichert, R. Schennach, Analysis of lignin precipitates on ozone treated kraft pulp by FTIR and AFM, Cellulose 19 (2012) 249–256.
[72] F.J. Schmied, C. Teichert, L. Kappel, U. Hirn, R. Schennach, Analysis of precipitated lignin on kraft pulp fibers using atomic force microscopy, Cellulose 19 (2012) 1013–1021.
[73] A. Quirk, J. Lipkowski, C. Vandenende, D. Cockburn, A.J. Clarke, J.R. Dutcher, et al., Direct visualization of the enzymatic digestion of a single fiber of native cellulose in an aqueous environment by atomic force microscopy, Langmuir 26 (7) (2010) 5007–5013.
[74] A. Rezanowich, D.A.I. Goring, Polyelectrolyte expansion of a lignin sulfonate microgel, J. Colloid Sci. 15 (1960) 452–471. http://dx.doi.org/10.1016/0095-8522(60)90049-0.
[75] E. Fratini, M. Bonini, A. Oasmaa, Y. Solantausta, J. Teixeira, P. Baglioni, SANS analysis of the microstructural evolution during the aging of pyrolysis oils from biomass, Langmuir 22 (2010) 306–312.
[76] H. Yoshida, R. Mörck, K.P. Kringstad, Fractionation of Kraft lignin by successive extraction with organic solvents. II. Thermal properties of Kraft lignin fractions, Holzforsching 41 (3) (1987) 171–176.
[77] R.C. Sun, J. Tomkinson, G.L. Jones, Fractional characterization of ash-AQ lignin by successive extraction with organic solvents from oil palm EFB fibre, Polym. Degrad. Stabil. 68 (2000) 111–119.
[78] S.W. Shalaby, Thermoplastic polymers, in: E.A. Turi (Ed.), Thermal Characterization of Polymeric Materials, Academic Press, New York, 1981.
[79] M. Tanahashi, T. Aoki, T. Higuchi, Dehydrogenative polymerization of monolignols by peroxidase and H_2O_2 in a dialysis Tube. II. Estimation of molecular weights by thermal softening method, Holzforshung 36 (3) (1982) 117–122.
[80] S. Baumberger, P. Dole, C. Lapierre, Using transgenic poplars to elucidate the relationship between the structure and the thermal properties of lignins, J. Agric. Food Chem. 50 (2002) 2450.
[81] W.O.S. Doherty, P. Mousavioun, C.M. Fellows, Value-adding to cellulosic ethanol: Lignin polymers, Ind. Crops Prod. 33 (2011) 259–276.
[82] F.D. Hileman, L.H. Wojcik, J.H. Futrell, I.N. Einhorn, Comparison of the thermal degradation products of α-Cellulose and Douglas fir under inert and oxidative environments, in: F. Shafizadeh, K.V. Sarkanen, D.A. Tillman (Eds.), Thermal Uses and Properties of Carbohydrates and Lignins, Academic Press, New York, 1976.
[83] M.J. Antal, Effects of reactor severity on the gas-phase pyrolysis of cellulose- and Kraft lignin-derived volatile matter, Ind. Eng. Chem. Prod. Res. Dev. 22 (1983) 366–375.
[84] M. Brebu, C. Vasile, Thermal degradation of lignin–A review, Cellul. Chem. Technol. 44 (9) (2010) 353–363.